

## Torque ripple minimization of direct torque controlled four phase switched reluctance motor using artificial intelligent controller

Pushparajesh Viswanathan<sup>1\*</sup>, Manigandan Thathan<sup>2</sup>

<sup>1</sup> Kongu Engineering College, Perundurai, Erode-638 052, Tamil Nadu, India

<sup>2</sup> P. A. College of Engineering and Technology, Pollachi, Tamil Nadu, India

(Received July 30 2015, Accepted February 21 2016)

**Abstract.** This paper proposes a new control approach for torque ripple minimization of a Direct Torque Controlled switched reluctance motor drive using Neural Network controller. It is still a very important problem to determine vectors voltage space initially in the conventional DTC for optimizing the torque error. The conventional control technique adopted for torque control uses hysteresis controller where the response of the torque and its ripple are very sluggish at different operating condition. Hence this paper focuses on improving the torque and flux response by using the combination of Intelligent Controller with Direct Torque control technique which results in better speed regulation and reduced torque ripple even under non linear conditions. The Intelligent controller gives high control over motor torque and speed, reduces rise time as well as overshoot. The neural network controller based Direct torque control is simulated with MATLAB/SIMULINK. The observed results shows the torque ripple minimization in switched reluctance motor can guarantee that the speed settling time is comparatively minimum as well as it flux and torque response is superior to conventional PWM control. The efficiency of the drive mainly in terms of speed and torque ripple control is analyzed with new set of computational algorithm.

**Keywords:** direct torque control, speed regulation, switching table, torque ripple, voltage vectors

### 1 Introduction

Switched Reluctance drives based application has increased in the recent years because of its advantages such as simple mechanical structure, high torque to inertia ratio, adaptable to hazardous environment, high speed operation etc. Being special electrical machines family, switched reluctance motor has been used for high power and high speed application such as electric traction, rocket space launching, robotic neck movement and so on. Due to its advancement and reliability SRM drives are now replacing Conventional AC/DC drives. The primary limitations of the drive are that it has highly non-linear torque characteristics compared with other conventional motors, which produces noise and vibrations. Various control schemes are investigated to improve the drive efficiency in terms of minimized torque ripple and better speed response. Sahoo et al.<sup>[18]</sup> specified SRM magnetization characteristics are highly nonlinear, where torque is a coupled and complex function of the phase currents and rotor position. An improved DTC method is proposed to 3-phase SRM, where the difference between conventional DTC and the proposed DTC to SRM has been discussed elaborately<sup>[8, 25]</sup>. A new set of space vectors is proposed for improving the torque performance of SRM<sup>[4]</sup>. The low speed and high speed operation of 6/4 SRM for control of torque is observed in [5]. A Intelligent control theory for controlling the torque production of SRM drive is discussed in [3, 23]. A short flux pattern based DTC for four phase switched reluctance drive is proposed in [11, 20]. Husain<sup>[10]</sup> reduced the torque ripple using simple current profiling technique. The disadvantage of this is the requirement of new and expensive winding topology. Jinupun et al.<sup>[13]</sup> introduced the sensoreless torque control of SRM. A NEFCLASS

\* Corresponding author. E-mail address: pushparajesh.v@gmail.com

based Neuro Fuzzy Controller is Proposed for SRM drive to improve the torque response is discussed in [2]. Minimization of torque ripple in 8/6 SRM using fuzzy logic controller for constant dwell angles has been discussed in [22]. Wang et al.<sup>[15]</sup> had minimized the torque ripples by employing a Direct torque Control technique along with torque controller. The main drawback of this method is limited to low speed region. The control technique adopted by Zhen et al.<sup>[26]</sup> controled the nonlinear characteristics of the motor by adopting a controller. The stability of this method is based on the selection of the stopping time. Henquires et al.<sup>[9]</sup> reduce the torque ripple by using hybrid controller say neuro fuzzy compensation technique. Vujicic et al.<sup>[24]</sup> and Lee et al.<sup>[14]</sup> introduced a family of TSFs by using different secondary objectives, such as power loss minimization and drive constraint consideration. Sivaprakasam et al.<sup>[19]</sup> introduced novel DTC techniques to reduce the torque ripple and Mechanical vibration. Sozer et al.<sup>[21]</sup> introduced a new method to control the excitation parameters such as turn on, turn off and the magnitude of the current. Rekioua et al.<sup>[17]</sup> used the current sensor and the incremental position sensor along with hysteresis controller for minimization of torque pulsation in permanent motor synchronous motor. Jeyabharath et al.<sup>[12]</sup> suggested the control of torque and torque ripple by controlling the magnitude of the flux linkage as well as speed change in the stator flux vectors. Hulste et al.<sup>[6]</sup> used the current and the position variables for estimate the instantaneous torque value by means a look up table  $T(\theta, i)$  and a finite element analysis software. Abdelli<sup>[1]</sup> proposed modulated hysteresis controller to maintain constant switching frequency in order to reduce the torque pulsation in Induction motor. Zheng et al.<sup>[27]</sup> developed a fuzzy proportional integration differential (PID) controller to minimize to motor driving system. Gao et al.<sup>[7]</sup> discussed various control strategies in terms of both conventional and intelligent controllers to limit the torque ripple in switched reluctance motor drive.

There is no specific literature survey available for the implementation of intelligent controller along with DTC for four phase SRM Drive as it is difficult to implement. To overcome the limitations in the four phase SRM drive the proposed method adopts the Artificial Neural Network for minimizing the torque error results in selecting the voltage vectors in the DTC switching table to improve the torque and speed response over a wide speed range. In this method the torque error is minimized at the faster rate compared with the conventional techniques adopted for such nonlinear drive system. The computational time is also less in the proposed technique compared with conventional technique adopted for reducing the torque ripple of SRM drive. The sequence of the work is such that initially the mathematical model of the drive is carried out followed by the implementation of the DTC technique. In that the proposed DTC technique is discussed initially and then the modeling of the Neural Network is carried out. The modeling is followed by the simulation and results and ended with conclusion and references.

## 2 Mathematical model

The most important properties of the this drive are their nonlinear angular positioning parameters and nonlinear magnetic characteristics. Winding inductance, BACK EMF and torque, which rely on the rotor angle that causes nonlinear angular positioning parameters, while magnetic saturation is the main reason for nonlinear magnetic characteristics. The key modeling principle of SRM is based on the Magnetic-position curve, that show the relation between linking flux and current in different rotor angles. The complete mathematical model for the SRM including the magnetic and electrical equations would be achieved considering magnetic saturation. The appendix contains parameters for a four phase SRM model with eight stator poles and six rotor poles, which is used in this paper. The complete mathematical model for the SRM including the magnetic and electrical equations would be achieved considering magnetic saturation.

The voltage across the motor phases is

$$V_j = Ri_j + \frac{d\lambda_j(\theta, i_j)}{dt} + \frac{d\lambda_i}{dt}, \quad (1)$$

where  $V_j$ , stands for the  $j^{th}$  phase winding voltage,  $i_j$  for the  $j^{th}$  phase current,  $j$  for the linking flux,  $R$  for the ohmic resistance of the phase winding and  $\lambda$  for the flux leakage. The linking coupling between adjacent windings has been neglected.

The chain derivation formula yields

$$V_j = Ri_j + \frac{d\lambda_j(\theta, i_j)}{dt} \times \frac{di_j}{dt} + \frac{d\lambda_j(\theta, i_j)}{d\theta} \times \frac{d\theta}{dt} + \frac{d\lambda_i}{dt}, \quad (2)$$

where an  $\frac{d\lambda_j(\theta, i_j)}{dt}$  is the increasing inductance ( $L_{inc}$ ) and  $\frac{d\lambda_j(\theta, i_j)}{d\theta}$  is the back EMF coefficient ( $C_w$ ), both of which are dependent on current and rotor angular position.

Considering  $L_k$  as the flux leakage

$$\frac{d\lambda_i}{dt} = L_k \frac{di_j}{dt}. \quad (3)$$

Replacing symbols in the above equation

$$V_j = Ri_j + L_{inc} \times \frac{di_j}{dt} + C_w \times \omega + L_k \times \frac{di_j}{dt}. \quad (4)$$

The rotor mechanical kinetic equation can be listed under the function of electromagnetic torque  $T_e$  and load torque  $T_L$  based on mechanical law

$$T_e = J \times \frac{d^2\theta}{dt^2} + f \times \frac{d\theta}{dt} + T_L, \quad (5)$$

$$\omega = \frac{d\theta}{dt}, \quad (6)$$

$$\frac{d\omega}{dt} = \frac{1}{J}(T_e - T_L - f.\omega). \quad (7)$$

where  $T_e$  is the electromagnetic torque,  $T_L$  specifies Load torque,  $J$  is the moment of inertia,  $f$  is the friction ratio coefficient and  $\omega$  is angular speed.

### 3 Direct torque control

The production of torque in this drive follows the reluctance principle, where the phase operates independently and in succession. Because of the high non-linearity of the magnetic circuit the general expression for the phase torque is given by

$$T(\theta, i) \approx i \frac{\partial \phi(\theta, i)}{\partial \theta}, \quad (8)$$

where  $\theta$  is the rotor position angle,  $i$  is the phase current. It is noted that in the SRM unipolar drives are normally used and thus the current in a motor phase is always positive. Hence from Eq. (8), the sign of the torque is directly related to the current whereas a negative torque is produced by decreasing the stator flux amplitude with respect to the rotor position movement. The negative and positive value are defined as “flux deceleration” and “flux acceleration”. Hence, a new SRM control technique is defined as follows:

- (a) The stator flux linkage vector of the motor is kept within amplitude hysteresis bands.
- (b) During the stator flux vector acceleration or deceleration the torque can be controlled.

The control objective is achieved by selecting an appropriate voltage vector and also achieved by acceleration or deceleration of the stator flux vector relative to the rotor movement. It should be noted that unlike conventional DTC the torque magnitude is also a product of the instantaneous current. However a similar phenomenon to that seen in conventional DTC may be found in this control scheme. As mentioned above, the conventional ac machine DTC due to a first order delay relative to the change in stator flux. Similarly in the SR control scheme, the stator current can be found to have a first order delay relative to the change in stator flux. Thus, it can be assumed that the current is relatively constant during the control of the flux acceleration and deceleration.

Therefore unlike the conventional ac motor DTC, each phase can have three states, leading to a total of 81 possible configurations.. These voltage state vectors are defined to lie in the center of eight zones, where

Table 1: Switching Function Table

Switching stage of power converter	Terminal voltage of winding	Switching function $S$
$V_1$ and $V_2$ both on	positive voltage	1
$V_1$ and $V_2$ one on and the other off	zero voltage	0
$V_l$ and $V_2$ both off	negative voltage	-1

each zone has a width of radians. One of the states is selected among the eight possible states at a time in order to keep the stator flux linkage and the motor torque within hysteresis bands. The switching function table and its principle of the switching stage is defined as below. According to the sections of instantaneous composition flux linkage, the selection of switching voltage vectors are as follows: supposed that the motor rotates at the anticlockwise direction and the composition flux linkage of stator lies in the  $k^{th}$  region ( $k = 1, \dots, 8$ ), and the motor runs at the driving mode. If the flux linkage  $\varphi$  is increased, then the switching voltage vector should be selected as  $V_{k-l}, V_{k+l}$ . On the contrary, to decrease the flux linkage  $\varphi \downarrow$ , the switching voltage vector should be selected as  $V_{k-3}, V_{k+3}$ . If to increase the torque  $T \uparrow$ , the switching voltage vector should be selected as  $V_{k+l}, V_{k+3}$ . On the contrary, if to decrease the torque  $T \downarrow$ , the switching voltage vector should be selected as  $V_{k-l}, V_{k-3}$ . Considering the requirement of flux linkage and torque, the switching table can be depicted as Tab. 2, where the upward arrow means to increase and the downward arrow means to decrease.

Table 2: Switching table of SRM

$T \uparrow \psi \uparrow$	$T \uparrow \psi \downarrow$	$T \downarrow \psi \uparrow$	$T \downarrow \psi \downarrow$
$V_{k+l}$	$V_{k-3}$	$V_{k-l}$	$V_{k+3}$

### 3.1 Proposed dtc control

Due to inherent nonlinear magnetic and saliency pole nature the torque developed in switched reluctance drive is well differentiated by great oscillations, even in case of constant phase excitation current. In this paper, the torque ripple is reduced by choosing the appropriate voltage switching vectors from the vector table using neural network controller.

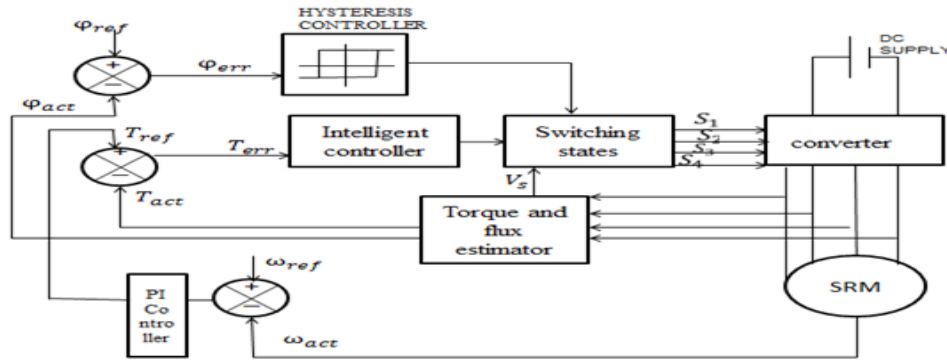


Fig. 1: Proposed block diagram

The block diagram of the proposed system under study is shown in Fig. 1. It consists of an drive with its power electronics converter and power supply. Different control strategies such as Voltage control, PI and PID control, and hysteresis control, can be used for the control of an SRM. However, these control techniques produce more vibrations, noise and also cause difficult to control the speed. Therefore, more advanced control techniques are used to overcome the limitations and improve the performance of the drive. Hence, controller based Direct Torque Control technique is studied and a Neural Network based controller is proposed. The

operation of a neuro controller is to optimize the error output from a comparator which compares the reference torque and the motor actual torque. The minimized torque and the flux output along with sector is used to select the optimum voltage sector which in turn generate the firing pulses for the controlled converter. The drive is tested under constant load and at different speed conditions: Initially, the motor is tested against its rated speed with a load torque of 2Nm. Second, the motor speed is suddenly decreased to 50% of its rated value with the above mentioned load torque followed by a removal of the disturbance after the motor reaches its steady state speed. Lastly the speed is further reduced to 25% of its rated speed with 2Nm load torque and the performance of the motor is observed.

### 3.2 Modeling of neuro controller

In classic DTC the stator voltage selection is made by hysteresis comparators with torque and flux magnitude errors as inputs and a predesigned gate-pulses look-up table that selects the stator voltage vector corresponding to the desired action. This control strategy from full negative torque to full positive leads to changes that cause high torque ripple. Due to slow rotor flux dynamics, the easiest way to change the load angle is to force a change in the stator flux vector by the application of the appropriate stator voltage vector vs. The capability to actuate an torque greatly depends on the e mf,  $\omega_m$ ,  $\psi_s$ . This means that ripple frequency varies with rotor speed obtaining variable switching frequency and a wide spectrum for torque and stator current. The structure of Neural Network is shown in Fig. 2. The input to the Neuro compensator is the error torque taken from comparators which compare the actual torque and the reference torque obtained from the conventional PI controller. The status Signal along with the flux signal is used to select the voltage vectors based on which the conventional asymmetric converters are operated. The Back Propagation Neuro compensator is with torque input comprising of ten linguistic rules with triangular form membership functions. The Data for training in Neuro compensator is collected from simulations of SRM control and output from the compensator is varied in terms of change in speed of SRM. The rule consequents are adjusted by a Intelligent controller algorithm consist of the combination of least square minimization and back propagation which is the training procedure followed here. The dc component at each learning iteration is removed in order to avoid the ripple compensator changing the output mean value of the torque. The error minimized output from the conventional PI controller which is refereed as Reference torque is compared with the actual torque. Here, supervised learning algorithm is utilized for training the neural network. There are number of supervised learning algorithm, here back propagation feed forward algorithm is used.

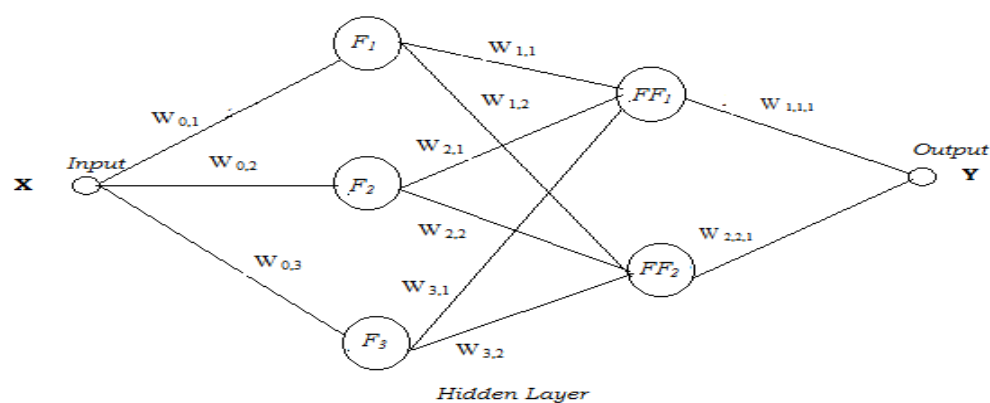


Fig. 2: Structure of neural network

The torque from the comparator is fed as the input to the Neuro compensator whose output target is error free torque signal. This status signal is used to select the voltage vectors from the vector table. The total number of datas used for this network is 100 in which 80 sets are used for training and the rest are used for testing purposes. The network has an input layer and the output layer along with two hidden layers. The

number of epochs that the network used for obtaining the best validation performance is 87. The Training data are obtained from simulations of steady-state simulation operation of the Switched reluctance drive system.

The DC component is removed from the motor torque at each learning iteration and only the remaining available is the ripple. This training data which is the torque ripple is tabulated against the reference torque and the angular position of the rotor. The training algorithm processes the training data to obtain the torque ripple which is interpreted as error information for each pair. The torque ripple error is reduced by readjusting the output of the Neuro compensator, and the process is continued until the minimum the torque ripple limit is achieved.

First collect the input and output data by running the simulation, then using that input and output train the neural network. The samples of input and output data are as follows:

Table 3: The samples of input and output data

Input	Output
710	532.4
727	547
740.6	555.2
758.3	570.9
771.6	578.4
788.5	601.4
805	606.2
822.5	614.7
838.4	623.6
855	540.3

Step 1. Type nn tool in the command window

Step 2. Neural network /data manager block will open. In that click new

Step 3. Create network or data block will open where select the input and output data

Step 4. Then click create.

Step 5. double click on the network name displayed in Neural network /data manager. Then new window will open in that click train menu to train the network.

Step 6. click export in the Neural network /data manager block. Select all and click export in the export from network /data manager block.

Step 7. Type gensim ('file name'). neural network block will open, then place the block in required location in Simulink.

The best performance is occurred at 13<sup>th</sup> epoch with the value of 4.0625e-007 which is very precise and based on these the error is termed to be zero. The gradient value and the Mu value at 13<sup>th</sup> epoch are 1.414e-006 and 1e-006. As the error is minimized at the earlier epoch which results in proper switching of devices causes the reduction of torque ripple and improves the performance of the switched reluctance motor drive. As the better performance is obtained at the minimum epoch the computational time is less and efficiency of the system is also improved.

#### 4 Simulation and results

A 4-phase 8/6 SRM as a prototype motor issued in simulation by MATLAB/SIMULINK environment. The load torque is taken as 2 Nm and the speed of SRM is 3000 RPM. In this work, Artificial Neural Network (ANN) Controller is employed to minimize the torque ripples in switched reluctance motor. The Hystersis Controller, conventional PI controller and Fuzzy Controller is also considered for comparison sake. The simulation is carried out for 1 seconds. For clarity over the responses, the time scale variation for flux linkages, 4 phase currents and total torque is taken as 0.71-0.76 second and for Speed, it is taken as 0-1 second. Fig. 3

shows the torque profile of the four phases of SRM Drives for 25% of the rated torque where the torque ripple is comparatively minimized compared to conventional controller. Fig. 4 shows the torque response for 50% of the rated torque and the response in terms of speed and torque is quite superior compared to other controllers. Fig. 5 depicts the torque response for 75% and Fig. 6 shows the torque response for a 100% of the rated torque. The motor performance under external disturbance is shown in Fig. 6. From the stimulated output the torque ripple along with speed and torque response is smoother compared to the conventional controller. It may be observed that the ANN based DTC minimize the torque ripples and also the settling time compared to the conventional and fuzzy controllers. Fig. 7 shows the torque response under external disturbances. The band limitation of a torque transducer can be avoided by using total torque and phase torque obtained from the torque estimator. Fig. 8 shows the speed response at various load conditions which shows the settling time of speed is faster compared to the conventional controller. Fig. 9 shows the current and torque profile for a load torque of 2Nm. The command speed response is very fast, typically, a few stroke angles. The torque-ripple minimization is maintained during the dynamic condition by the proposed algorithm. The tuning constants were determined and optimized using the optimization techniques through simulation. The algorithm computation time for one cycle plays a significant role in dictating the amount of torque ripple present at an appropriate speed. The significance is even greater than the resolution of the position feedback signal. In Tab. 4, the statistical parameters such as torque ripple in Nm and torque ripple in percentage along with the settling time for various controllers are reported. It also shows the standard deviation of total torque ( $T$ ) and settling time ( $t_s$ ) of the responses. For the PI speed controller, which lies in outer loop, the proportional and integral gain ( $K_p$ ,  $K_i$ ) has been taken as 1.863 and 0.069 respectively. These parameters are obtained by means of using graphical tuning (bode plot) method which is available in control design tools of MATLAB/SIMULINK environment. These parameters are well tuned to yield better results for torque ripple reduction than without controller. Results reveal that mean torque is increased and the torque ripple coefficient and standard deviation of total torque ( $T$ ) are reduced for Neural Network controller.

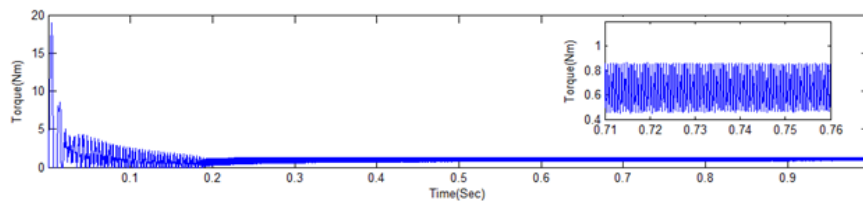


Fig. 3: Motor torque response for a 25% of the rated torque

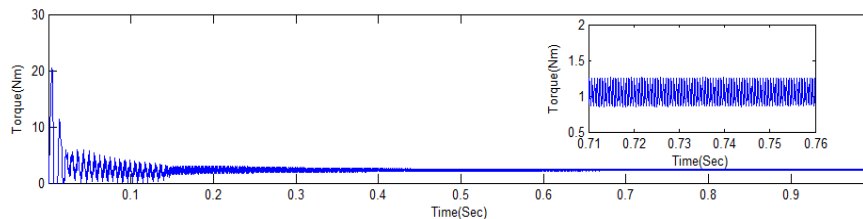


Fig. 4: Motor torque response for 50% of the rated torque

In FL controller, torque ripple coefficient is reduced than PI controller and Hysteresis Controller. But in ANN, it is still decreased when compared with PI controller and with FL controller. The settling time is also improved in both cases but ANN has better performance when compared with PI controller and FL. The reduced torque ripple, quick torque response with torque ripple minimized of nearly about 7% using the Neural Network Controller based DTC compared to the conventional PI and Hysteresis controller. The

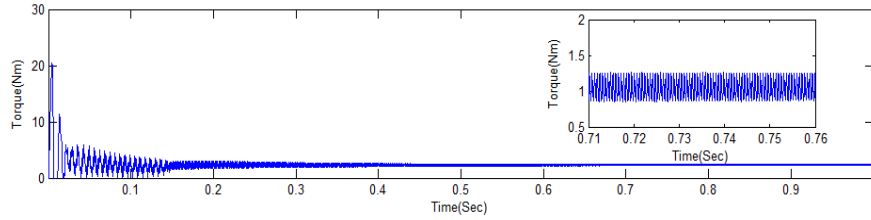


Fig. 5: Motor torque response for a 75% of the rated torque

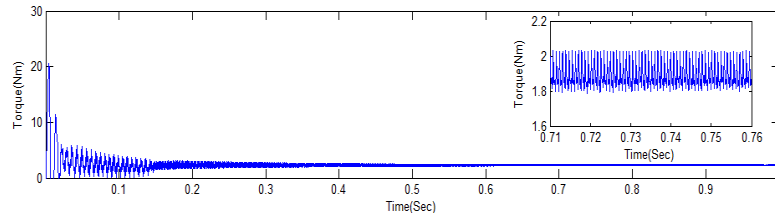


Fig. 6: Motor torque response for a 100% of the rated torque

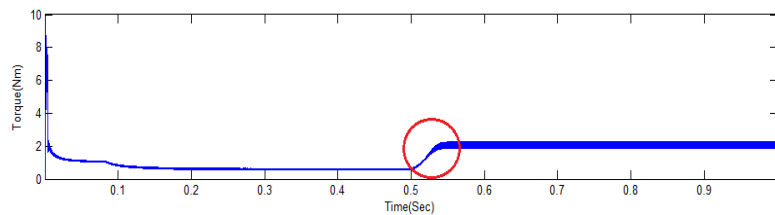


Fig. 7: Motor response under external load disturbances

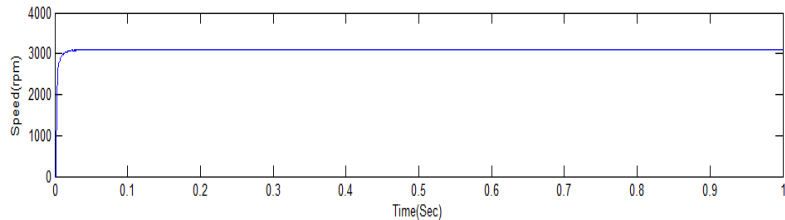


Fig. 8: Motor speed response for 100% of the rated speed

Computation period for one cycle should get completed within the encoder time period at the higher speeds of the application to obtain the best results.

## 5 Experimental results

In addition to the simulation results, the proposed DTC method is experimentally tested to verify the effectiveness of the proposed methods. The experimental arrangement of the proposed system is same as that of Fig. 2. A 1 kW SRM is used for this experimental verification. Fig. 14 shows the experimental arrangement of the proposed system. The input for the insulated gate bipolar transistor which is used as an inverter is fed from a four phase intelligent power module. The SPARTAN 3A/3A DSP FPGA board is used to generate the gating pulses which are fed as the input to the inverter. The experimental results are taken with help of a Tektronix TDS 2004B digital storage oscilloscope. In addition to the simulation results, the proposed method is experimentally tested to verify the effectiveness of the proposed methods. The experimental arrangement of the proposed system is same as that of Fig. 1. The switching pulse pattern for a load torque of 2Nm with a rated speed of 3000 rpm is shown in Fig. 1. The voltage profile and the current profile for 100% of the load torque is shown in Figs. 11 and 12. The experimental results for the proposed method for a load of 2Nm and



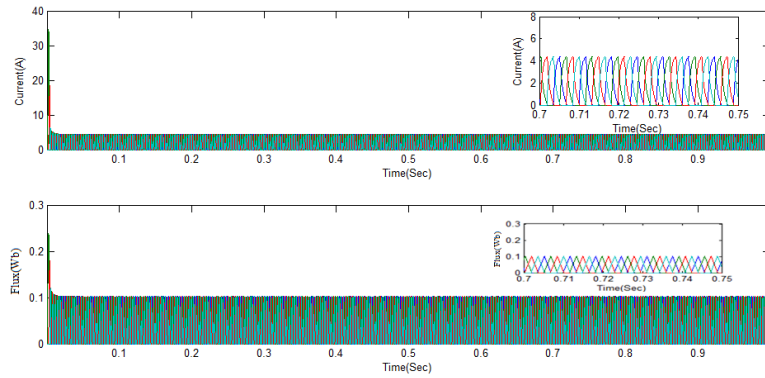


Fig. 9: Motor current and flux response for 100% of the load torque

a speed of 3000 rpm is shown in Fig. 13. Experimental results were also taken to evaluate robustness against external load disturbances. From the experimental results, the RMS torque ripple of the proposed DTC method is 0.285 Nm whereas for the same method 0.205 Nm is obtained from the simulation. The experimental setup still demands improvements in the area of digital implementation. If this is achieved the proposed DTC method is supposed to have performance similar to the results obtained in the simulation.

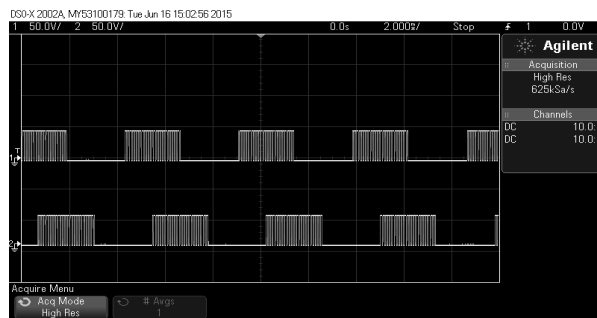


Fig. 10: Switching pulse pattern for a load torque of 2 Nm

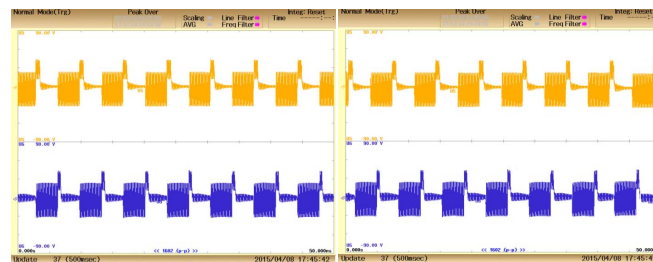


Fig. 11: Voltage profile for a load torque of 2 NM

## 6 Conclusion

The performance of the neural network optimization technique is comparatively evaluated with conventional torque control techniques and existing literatures. Simulation results prove that the proposed Neural Network algorithm is able to reduce the torque ripple in the range of about 1.5% to 2% at different operating conditions compared to convention methods. The settling time of the torque and the response time of the speed

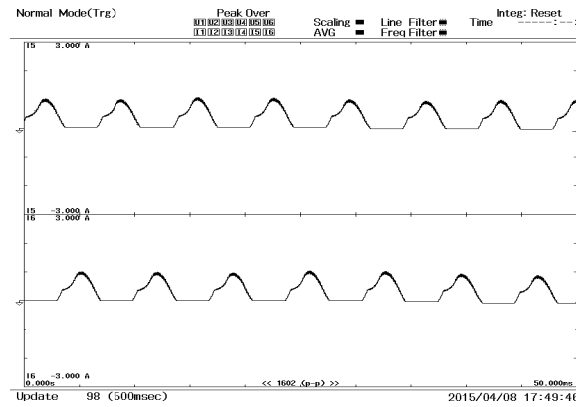


Fig. 12: Current profile for a load torque of 2 Nm

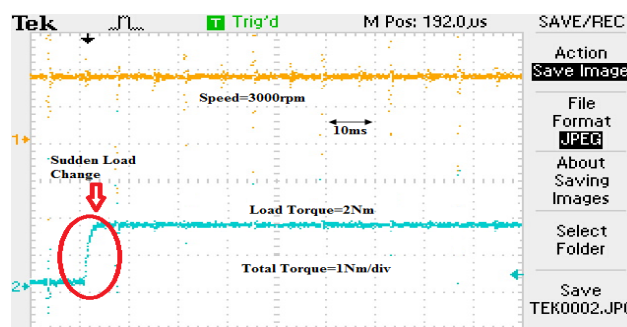


Fig. 13: Phase torque response for a load torque of 2Nm and a speed of 3000rpm

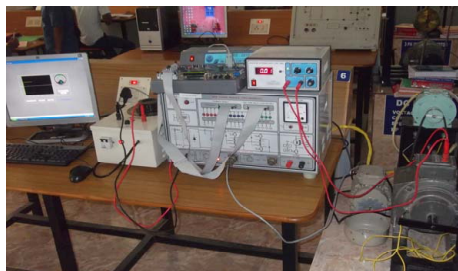


Fig. 14: Experimental setup of a 1 kW SRM with controller

Table 4: Specification of SRM

Parameter	Value
Type	8/4
No. of phases	4
Voltage	120 V
Maximum current	24 A
Stator resistance	0.96 ohm
Unaligned inductance	10 mH
Aligned inductance	49 mH
Inertia	0.008 Kg·m <sup>2</sup>
Friction	0.001 N·m·s
Max.flux linkage	0.3 V·s

is also reduced in the proposed technique compared classical controller which in turn increases the efficiency of the drive. The computational time is calculated as 3.17s which is comparatively superior compared with other intelligent controller. The torque response is absolutely faster and it is 0.06s in the experimental which is similar to the response time of 0.05s obtained in simulation.

## References

- [1] R. Abdelli, D. Rekioua, T. Rekioua. Performances improvements and torque ripple minimization for vsi fed induction machine with direct control torque. *ISA transactions*, 2011, **50**(2): 213–219.
- [2] M. A. Akcayol, C. Elmas. Nefclass-based neuro fuzzy controller for srm drive. *Engineering Applications of Artificial Intelligence*, 2005, **18**(5): 595–602.
- [3] S. Bolognani, M. Zigliotto. Fuzzy logic control of a switched reluctance motor drive. *Industry Applications, IEEE Transactions on*, 1996, **32**(5): 1063–1068.
- [4] A. D. Cheok, Y. Fukuda. A new torque and flux control method for switched reluctance motor drives. *Power Electronics, IEEE Transactions on*, 2002, **17**(4): 543–557.
- [5] A. D. Cheok, P. H. Hoon. A new torque control method for switched reluctance motor drives. **in: Industrial Electronics Society, 2000. IECON 2000. 26th Annual Conference of the IEEE**, vol. 1, IEEE, 2000, 387–392.
- [6] F. Dhulster, K. Stockman, R. Belmans. Modelling of switched reluctance machines: state of the art. *International Journal of Modelling and Simulation*, 2004, **24**(4): 216–223.
- [7] X. Gao, X. Wang, et al. A review of torque ripple control strategies of switched reluctance motor. *International Journal of Control and Automation*, 2015, **8**(4): 103–116.
- [8] H.-J. Guo. Considerations of direct torque control for switched reluctance motors. **in: Industrial Electronics, 2006 IEEE International Symposium on**, vol. 3, IEEE, 2006, 2321–2325.
- [9] L. Henriques, L. Rolim, et al. Torque ripple minimization of switched reluctance drive using a neuro-fuzzy control technique. *IEEE Transactions on Magnetics*, 2000, **36**.
- [10] I. Husain. Minimization of torque ripple in srm drives. *industrial electronics, IEEE Transactions on*, 2002, **49**(1): 28–39.
- [11] B. Jeong, K. Lee, et al. Direct torque control for the 4-phase switched reluctance motor drives. **in: Electrical Machines and Systems, 2005. ICEMS 2005. Proceedings of the Eighth International Conference on**, vol. 1, IEEE, 2005, 524–528.
- [12] R. Jeyabharath, P. Veena, M. Rajaram. A novel dtc strategy of torque and flux control for switched reluctance motor drive. **in: Power Electronics, Drives and Energy Systems, 2006. PEDES'06. International Conference on**, IEEE, 2006, 1–5.
- [13] P. Jinupun, P. C.-K. Luk. Direct torque control for sensorless switched reluctance motor drives. **in: Power Electronics and Variable Speed Drives, 1998. Seventh International Conference on (Conf. Publ. No. 456)**, IET, 1998, 329–334.
- [14] D.-H. Lee, J. Liang, et al. A simple nonlinear logical torque sharing function for low-torque ripple sr drive. *Industrial Electronics, IEEE Transactions on*, 2009, **56**(8): 3021–3028.
- [15] W. Mianhua. Four phase switched reluctance motor direct torque control. **in: Measuring Technology and Mechanics Automation (ICMTMA), 2011 Third International Conference on**, vol. 2, IEEE, 2011, 251–254.
- [16] T. Miller. *Switched Reluctance Motors and their Control*. Magna Physics & Oxford, 1993.
- [17] T. Rekioua, D. Rekioua. Direct torque control strategy of permanent magnet synchronous machines. **in: Power Tech Conference Proceedings, 2003 IEEE Bologna**, vol. 2, IEEE, 2003, 6–pp.
- [18] S. K. Sahoo, S. Dasgupta, et al. A lyapunov function-based robust direct torque controller for a switched reluctance motor drive system. *Power Electronics, IEEE Transactions on*, 2012, **27**(2): 555–564.
- [19] A. Sivaprakasam, T. Manigandan. An alternative scheme to reduce torque ripple and mechanical vibration in direct torque controlled permanent magnet synchronous motor. *Journal of Vibration and Control*, 2013, 1077546313492182.
- [20] G. Song, Z. Li, et al. Direct torque control of switched reluctance motors. **in: Electrical Machines and Systems, 2008. ICEMS 2008. International Conference on**, IEEE, 2008, 3389–3392.
- [21] Y. Sozer, D. Torrey. Optimal turn-off angle control in the face of automatic turn-on angle control for switched-reluctance motors. *Electric Power Applications, IET*, 2007, **1**(3): 395–401.
- [22] P. Srinivas, P. Prasad. Torque ripple minimization of 8/6 switched reluctance motor with fuzzy logic controller for constant dwell angles. **in: Power Electronics, Drives and Energy Systems (PEDES) & 2010 Power India, 2010 Joint International Conference on**, IEEE, 2010, 1–6.
- [23] D. A. Staton, W. L. Soong, T. J. Miller. Unified theory of torque production in switched reluctance and synchronous reluctance motors. *Industry Applications, IEEE Transactions on*, 1995, **31**(2): 329–337.

- [24] V. P. Vujicic. Minimization of torque ripple and copper losses in switched reluctance drive. *Power Electronics, IEEE Transactions on*, 2012, **27**(1): 388–399.
- [25] X. Xue, K. Cheng, S. Ho. Optimization and evaluation of torque-sharing functions for torque ripple minimization in switched reluctance motor drives. *Power Electronics, IEEE Transactions on*, 2009, **24**(9): 2076–2090.
- [26] Z. Z. Ye, T. W. Martin, J. C. Balda. Modeling and nonlinear control of a switched reluctance motor to minimize torque ripple. **in:** *Systems, Man, and Cybernetics, 2000 IEEE International Conference on*, vol. 5, IEEE, 2000, 3471–3478.
- [27] L. Zheng, Y. Ren, et al. The investigation of control strategies of switched reluctance motor to reduce the torque ripple in vehicle. *Tech. Rep.*, SAE Technical Paper, 2015.